ISSN 2079-1704. Хімія, фізика та технологія поверхні. 2025. Т. 16. № 3. С. 406-413

PACS 81.05.Zx; 71.15.Mb; 82.30.-b doi: 10.15407/hftp16.03.406

D.B. Nasiedkin, A.G. Grebenyuk, L.F. Sharanda, Yu.V. Plyuto

MECHANISM OF MoO_3 DISPERGATION ON SiO_2 SURFACE

Chuiko Institute of Surface Chemistry of National Academy of Sciences of Ukraine
17 Oleg Mudrak Str., Kyiv, 03164, Ukraine, E-mail: dmytro.nasiedkin@isc.gov.ua

Molybdena dispergation on silica surface via heat treatment of dry mixtures of MoO_3 and the dispersed silica support is a convenient preparative technique of the synthesis of surface Mo(VI) oxo-species. The driving force for the thermally induced dispergation of bulk MoO_3 is the decrease in surface energy which is lower for surface Mo(VI) oxo-species. The aim of the present study is a quantum chemical modelling of the mechanism of MoO_3 molecule interaction with ≡Si–OH groups of silica surface via reaction $2(\equiv Si–OH) + MoO_3 \rightarrow (\equiv Si–O–)_2Mo(=O)_2 + H_2O$ resulting in the formation of $(\equiv Si–O–)_2Mo(=O)_2$ Mo(VI) oxo-species. Restricted Hartree-Fock method (MO LCAO approximation) using the SBKJC (Stevens-Basch-Krauss-Jasien-Cundari) valence-only basis set was used. $Si_{10}O_{12}(OH)_{16}$ cluster was used as a model for highly hydroxylated silica surface in which silicon atoms in the core siloxane chains are saturated by four silanol and six silanediol groups. Such a cluster was considered as providing a realistic structure for the SiO_2 surface and exhibiting high stability due to its large size. The optimised geometry of MoO_3 molecule of C_{3v} symmetry was used in calculations. Quantum chemical simulation of the reaction $Si_{10}O_{12}(OH)_{16} + MoO_3 \rightarrow Si_{10}O_{12}(OH)_{14}O_2MoO_2 + H_2O$ accompanied by the formation of surface $(\equiv Si–O–)_2Mo(=O)_2$ Mo(VI) oxo-species was undertaken. We considered two structures of $(\equiv Si–O–)_2Mo(=O)_2$ Mo(VI) oxo-species attached to $Si_{10}O_{12}(OH)_{16}$ silica cluster via nearby and distant ≡Si–OH groups. At 700 K, when molybdena dispergation over silica surface begins, the Gibbs energy of the formation of $(\equiv Si–O–)_2Mo(=O)_2$ Mo(VI) oxo-species via reaction of MoO_3 molecule with nearby and distinct ≡Si–OH groups of $Si_{10}O_{12}(OH)_{16}$ cluster was found to be -260 and -337 kJ/mol, respectively. The mechanism of the reaction of MoO_3 molecule with distant ≡Si–OH groups of $Si_{10}O_{12}(OH)_{16}$ cluster accompanied by the formation of $(\equiv Si–O–)_2Mo(=O)_2$ Mo(VI) oxo-species was considered as more favourable energetically. It has been found that at 700 K the reaction proceeds in two stages and requires overcoming of the activation barriers of 161 and 154 kJ/mol.

***Keywords**: quantum chemical simulation, silica, molybdena, surface dispergation, reaction mechanism*

INTRODUCTION

Molybdena dispergation on silica surface via heat treatment of dry mixtures of MoO_3 and the dispersed silica support is convenient preparative technique of the synthesis of surface Mo(VI) oxo-species. The driving force for the thermally induced dispergation of bulk MoO_3 is the decrease in surface energy which is lower for surface Mo(VI) oxo-species. Stabilization of surface Mo(VI) oxo-species occurs due to interaction with surface hydroxyl groups [1].

Numerous experimental studies of MoO_3 thermally induced dispergation over supports surface were undertaken [1]. They were focused on individual well-defined SiO_2 [2, 3], Al_2O_3 [3–6] or mixed SiO_2−Al_2O_3 [7, 8] supports, siliceous [9–11] and aluminosilicate [5, 6, 12] molecular sieves. Special attention was given to surface Mo(VI) oxo-species resulted from MoO_3 dispergation on aluminosilicate molecular sieves MCM-22, MCM-56 and 2D-MFI [13] and also on siliceous molecular sieves MCM-41, MCM-48 and SBA-15 [14, 15] because of their applicability in olefins metathesis. It was experimentally determined that the temperature of ca. 700–800 K is required for dispergation of MoO_3 over supports surface.

In the case of dispersed supports like Al_2O_3, SiO_2 or TiO_2 the gas phase diffusion mechanism where Mo oxide clusters are evaporated from MoO_3 crystallites with subsequent dispergation in monomeric state on the support surface was proposed [16, 17]. The diffusion process of MoO_3 on oxide thin films (Al_2O_3, SiO_2, TiO_2) was also investigated. During thermal treatment, MoO_3 diffused onto the surface of those films and formed a monolayer or a submonolayer. A possible explanation for all the phenomena is the combination of surface diffusion onto the surface of the support and transportation via the gas phase [18, 19].

The distribution of MoO_3 on the surface of dispersed supports is important from fundamental and applied points of view as plays a crucial role in the development of scientific basis of the rational design of supported

heterogeneous catalysts in chemical and petrochemical industry and in environmental control [20]. The catalytic metathesis of olefins is an example of the industrially important reaction where Mo(VI) oxo-species in atomically precise form play a central role [21–23].

The in-depth study of the structure of surface Mo(VI) oxo-species is the subject of standing interest using modern experimental techniques [24–28] and theoretical methods [29–32].

The aim of the present study is a quantum chemical modelling of the mechanism of MoO_3 molecule interaction with ≡Si–OH groups of silica surface via reaction $2(\equiv Si–OH) + MoO_3 \rightarrow (\equiv Si–O–)_2Mo(=O)_2 + H_2O$ resulting in the formation of $(\equiv Si–O–)_2Mo(=O)_2$ Mo(VI) oxo-species.

METHOD AND MODELS

The process of interaction between molybdena and silica surface was simulated using the Restricted Hartree-Fock method (MO LCAO approximation) with the PC GAMESS/Firefly QC package which is based on the GAMESS (US) [33, 34] source code. In order to shorten the computing time, the SBKJC (Stevens-Basch-Krauss-Jasien-Cundari) valence-only basis set was used which required application of respective effective core potential. The Gibbs energy ($\Delta G_{react.T}$) of the reaction $Si_{10}O_{12}(OH)_{16} + MoO_3 \rightarrow Si_{10}O_{12}(OH)_{14}O_2MoO_2 + H_2O$ resulting in the formation of the considered $(\equiv Si–O–)_2Mo(=O)_2$ species was calculated within 300–1100 K temperature interval using the formula:

$$\Delta G_{react.T} = [G_T(Si_{10}O_{12}(OH)_{14}O_2MoO_2) + G_T(H_2O)] - [G_T(Si_{10}O_{12}(OH)_{16}) + G_T(MoO_3)],$$

where $[G_T(Si_{10}O_{12}(OH)_{14}O_2MoO_2) + G_T(H_2O)]$ and $[G_T(Si_{10}O_{12}(OH)_{16}) + G_T(MoO_3)]$ are the calculated Gibbs energy of the formation of the products and reactants, respectively. The Gibbs energy of activation barriers was calculated as a difference between the Gibbs energy of the transition state and the corresponding previous ground state.

RESULTS AND DISCUSSION

The cluster $Si_{10}O_{12}(OH)_{16}$ was used in this work as a model of highly hydroxylated silica surface. The cluster starting geometry proposed in [35, 36] represents a structural fragment of a β-cristobalite crystal. Silicon atoms in the core siloxane chains are saturated by four silanol and six silanediol groups. Such $Si_{10}O_{12}(OH)_{16}$ cluster was considered as providing a realistic structure for the SiO_2 surface and exhibiting high stability due to its large size. It presents on its surface different types of hydroxyl groups that can act as adsorption and reactions sites and is also useful to model silica gel surface.

In the initial $Si_{10}O_{12}(OH)_{16}$ model composed of regular SiO_4 tetrahedra all Si–O bonds had the lengths of 1.700 Å and O–Si–O angles of 109.5° [37, 38]. After the geometry optimization they have slightly changed to 1.631–1.651 Å and 104.5–108.2°, respectively.

We considered two structures of $(\equiv Si–O–)_2Mo(=O)_2$ Mo(VI) oxo-species attached to $Si_{10}O_{12}(OH)_{16}$ silica cluster via nearby and distant ≡Si–OH groups of silica surface. They are shown in Fig. 1 and Fig. 2, respectively. The bond length and bond angles in the considered $(\equiv Si–O–)_2Mo(=O)_2$ Mo(VI) oxo-species are presented in Table 1.

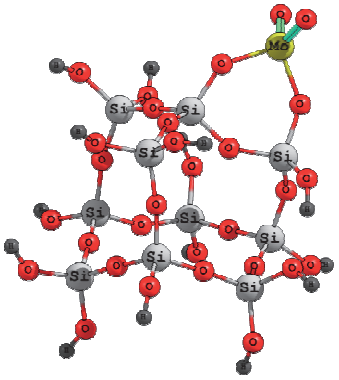

E_{tot} -584.56565 Hartree

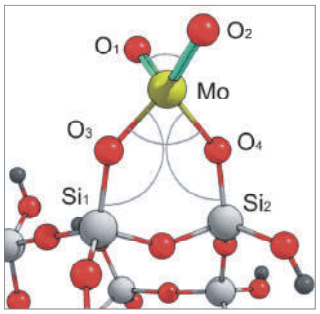

Fig. 1. Geometry optimized structures of $(\equiv Si–O–)_2Mo(=O)_2$ Mo(VI) oxo-species attached to $Si_{10}O_{12}(OH)_{16}$ silica cluster via nearby ≡Si–OH groups

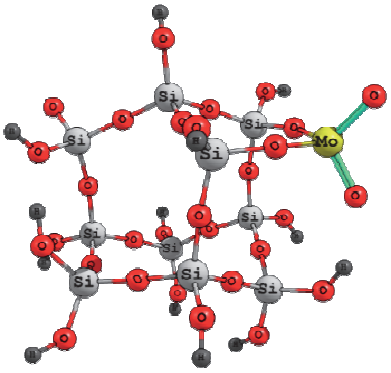

E_{tot} -584.60147 Hartree

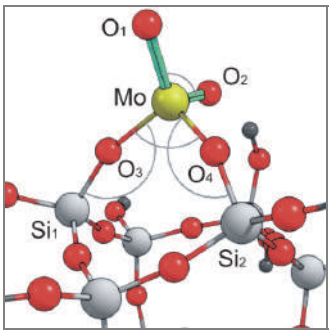

Fig. 2. Geometry optimized structures of (≡Si–O–)$_2$Mo(=O)$_2$ Mo(VI) oxo-species attached to $Si_{10}O_{12}(OH)_{16}$ silica cluster via distant ≡Si–OH groups

Table 1. Bond length and bond angles in the considered (≡Si–O–)$_2$Mo(=O)$_2$ Mo(VI) oxo-species

(≡Si–O–)$_2$Mo(=O)$_2$		**Bond length, Å**		
Mo(VI) oxo-species	Mo=O$_1$	Mo=O$_2$	Mo–O$_3$	Mo–O$_4$
a	1.683	1.685	1.883	1.879
b	1.683	1.683	1.851	1.857
(≡Si–O–)$_2$Mo(=O)$_2$		**Bond angle, °grad**		
Mo(VI) oxo-species	O$_1$=Mo=O$_2$	O$_3$–Mo–O$_4$	Mo–O$_3$–Si$_1$	Mo–O$_4$–Si$_2$
a	109.0	94.8	138.8	139.2
b	108.8	102.0	158.8	159.9

In Table 1, the structure *a* corresponds to (≡Si–O–)$_2$Mo(=O)$_2$ Mo(VI) oxo-species attached to $Si_{10}O_{12}(OH)_{16}$ silica cluster via nearby ≡Si–OH groups while structure *b* corresponds to oxo-species attached to $Si_{10}O_{12}(OH)_{16}$ silica cluster via distant ≡Si–OH groups. The structure *b* appeared to be more energetically favourable (E_{tot} -584.60147 Hartree) in contrast to structure *a* (E_{tot} -584.56565 Hartree).

The Mo=O bond length in (≡Si–O–)$_2$Mo(=O)$_2$ Mo(VI) oxo-species *a* and *b* is almost the same and varies in the range of 1.683–1.685 Å. This also concerns the O=Mo=O angle which is in the range of 108.8–109.0° and is very close to theoretical value of 109.5° in tetrahedral coordination. The main difference is observed for O–Mo–O angle in (≡Si–O–)$_2$Mo(=O)$_2$ Mo(VI) oxo-species which for the structures *a* and *b* was found to be of 94.8° and 102.0°, respectively. The observed O–Mo–O angle in the structures *a* appeared to be more distorted in comparison with that in the structures *b*. This correlates with higher energetic favourability of the structure *b* in comparison with the structure *a* due to a less bond angle straining.

We calculated the temperature dependences of the Gibbs energy of the reaction $Si_{10}O_{12}(OH)_{16} + MoO_3 = Si_{10}O_{12}(OH)_{14}O_2MoO_2 + H_2O$ which can result in the formation of (≡Si–O–)$_2$Mo(=O)$_2$ Mo(VI) oxo-species (structures *a* and *b*).

The optimized geometry of MoO_3 molecule (E_{tot} = -114.23859 Hartree) of C_{3v} symmetry had the Mo=O bond length of 1.708 Å and the bond angle O=Mo=O of 114.9°. The calculated values of geometric parameters of MoO_3 model are close to the analogous values obtained earlier. HF SCF calculations [39] yielded a Mo=O bond length of 1.682 Å and showed that the molecule is nonplanar with Mo=O bonds forming an angle of 105° with the C_3 axis. After correlation corrections, the values 1.766 Å and 112°, respectively, were obtained for these parameters. By DFT calculations, a Mo=O bond length was found to be of 1.734 Å and the bond angle O=Mo=O of 108.0° [40].

It appears to be close to experimental values of MoO_3 molecule of C_{3v} symmetry with the bond length of 1.711±0.008 Å and the bond angle O=Mo=O of 112±8° obtained from the electron diffraction investigation in the vapour phase [41]. A pyramidal C_{3v} structure for

gaseous MoO_3 was also suggested from the infrared spectrum [42] with a Mo=O bond length of 1.73 Å.

The undertaken simulation of the reaction of MoO_3 molecule with $Si_{10}O_{12}(OH)_{16}$ cluster showed that the formation of both $(\equiv Si–O–)_2Mo(=O)_2$ Mo(VI) oxo-species (structures *a* and *b*) were energetically favourable. For the temperature interval of 300–1100 K, the Gibbs energy of the reaction resulting in the formation of the structure *a* varies from -276 to -243 kJ/mol, respectively. The Gibbs energy of the reaction resulting in the formation of the structure *b* varies from -368 to -303 kJ/mol with the temperature increase from 300 to 1100 K.

At 700 K, when molybdena dispergation over silica surface begins, the Gibbs energy of the reaction of the formation of $(\equiv Si–O–)_2Mo(=O)_2$ Mo(VI) oxo-species of type *a* and *b* structure was found to be -260 and -337 kJ/mol, respectively. As the appearance of $(\equiv Si–O–)_2Mo(=O)_2$ Mo(VI) oxo-species of type *b* structure is more energetically favourable, the mechanism of their formation was considered.

Quantum chemical modelling of the mechanism of MoO_3 molecule interaction with ≡Si–OH groups of silica surface was done using the initially optimized structure of $Si_{10}O_{12}(OH)_{16}$ silica cluster and MoO_3 molecule. Fig. 3 shows the stages of proposed mechanism of MoO_3 molecule reaction with ≡Si–OH groups of silica surface resulted in the formation of $(\equiv Si–O–)_2Mo(=O)_2$ Mo(VI) oxo-species of type *b*.

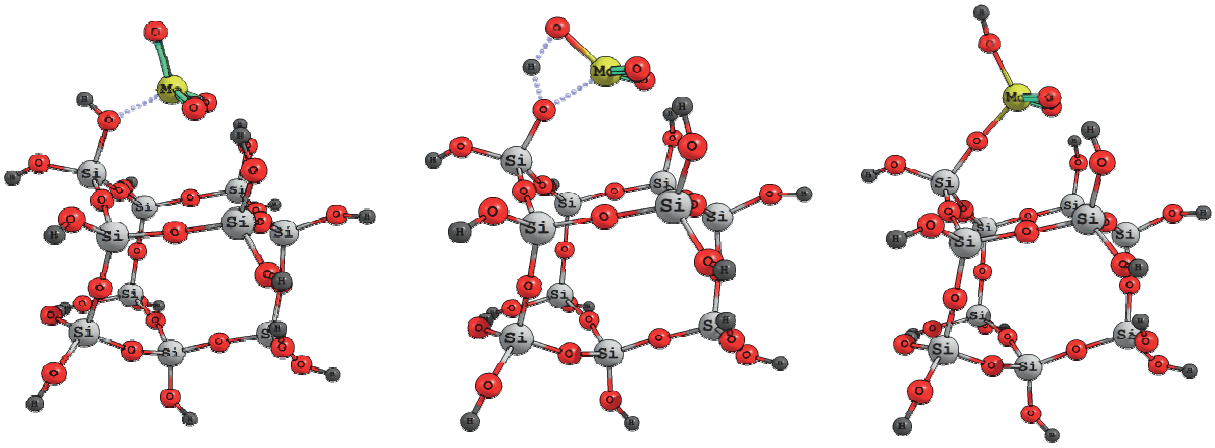

2
E_{tot} -601.39078 Hartree

3 (TS1)
E_{tot} -601.32582 Hartree

4
E_{tot} -601.43828 Hartree

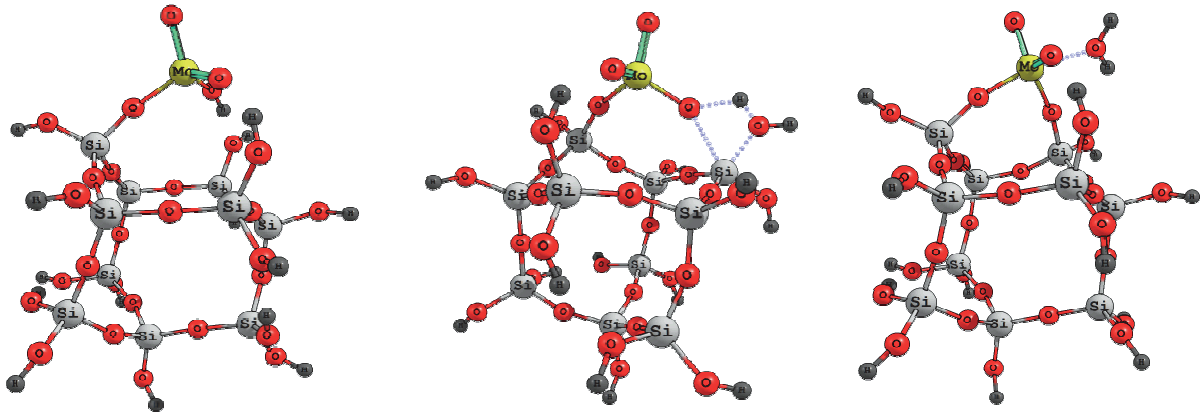

5
E_{tot} -601.44529 Hartree

6 (TS2)
E_{tot} -601.39180 Hartree

7
E_{tot} -601.44545 Hartree

Fig. 3. The proposed mechanism of MoO_3 molecule reaction with ≡Si–OH groups of silica surface resulted in the formation of $(\equiv Si–O–)_2Mo(=O)_2$ Mo(VI) oxo-species of type *b*

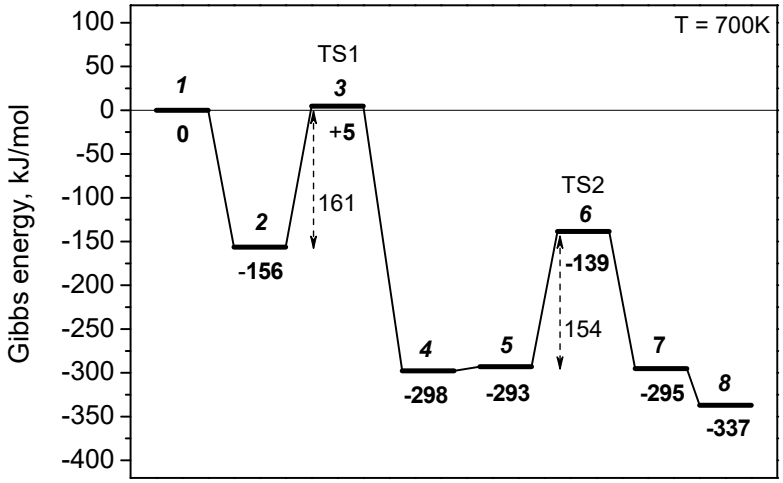

Fig. 4. Changes in Gibbs energy along the reaction pathway of the formation (≡Si–O–)$_2$Mo(=O)$_2$ Mo(VI) oxo-species via chemical reaction of MoO_3 molecule with ≡Si–OH groups of silica surface at 700 K

Fig. 4 demonstrates the changes in Gibbs energy along the reaction pathway of the formation (≡Si–O–)$_2$Mo(=O)$_2$ Mo(VI) species oxo-species via chemical reaction of MoO_3 molecule with ≡Si–OH groups of silica surface at 700 K. Numbers in italic bold and abbreviations of the transition states TS1 and TS2 in Fig. 4 correspond to those in Fig. 3. The Gibbs energy of the initial structure *1* in Fig. 4 (not shown in Fig. 3 for simplification) is the sum of the Gibbs energies of the individual cluster $Si_{10}O_{12}(OH)_{16}$ and MoO_3 molecule and was chosen to be zero for the analysis of changes of Gibbs energies along the reaction pathway.

The proposed sequence of the reactions steps resulted in the formation of (≡Si–O–)$_2$Mo(=O)$_2$ Mo(VI) oxo-species are as follows.

We have found out that the reaction begins from coordination of molybdenum atom of MoO_3 molecule to oxygen atom of ≡Si–OH group. The formation of coordination Mo···O bond in ground-state (structure *2*) is accompanied by reducing of the relative Gibbs energy of the system to -156 kJ/mol. The length of the coordination bond Mo···O in the structure *2* is 2.104 Å and decreases to 2.033 Å in the transition state TS1 (structure *3*).

The next ground-state structure *4* appears due to a transfer of the proton of ≡Si–OH group to the oxygen atom of MoO_3 molecule and the formation ≡Si–O–Mo(=O)$_2$–OH group (the system relative energy decreases to -298 kJ/mol). The length of the covalent Mo–O bond in the ground state (structure *4*) was found to be 1.840 Å. This process requires overcoming of the activation barrier of 161 kJ/mol via transfer of the proton of ≡Si–OH group to the oxygen atom of MoO_3 molecule in more complex structure *3* where oxygen atom of MoO_3 molecule is additionally coordinated to hydrogen atom of ≡Si–OH group in TS1 with relative energy of +5 kJ/mol.

Further, rearrangement of structure *4* assumes practically barrier-free rotation around the Mo–O bond (ground-state, structure *5*) and the relative energy slightly increases up to -293 kJ/mol. In the structure *4*, a weak interaction is observed between oxygen atoms of two Mo=O groups and hydrogen atoms of ≡Si–OH groups with hydrogen bond length of 2.086 and 2.009 Å. In structure *5*, the oxygen atom of Mo=O group exhibits a weak interaction with hydrogen atom of ≡Si–OH group (hydrogen bond length of 1.967 Å) and hydrogen atom of ≡Si–O–Mo(=O)$_2$–OH group –with oxygen atom of ≡Si–OH group (hydrogen bond length of 1.627 Å).

Reaction of ≡Si–O–Mo(=O)$_2$–OH group with ≡Si–OH group results in the formation of (≡Si–O–)$_2$Mo(=O)$_2$ group and H_2O molecule (ground-state, structure *7*) and the system relative energy slightly increases up to -295 kJ/mol. This step is accompanied by overcoming an activation barrier of 154 kJ/mol in TS2 (structure *6* with relative energy of -139 kJ/mol). In the transition state TS2 (complex transition structure *6*), we observe the distance between the oxygen atom of Mo–OH

group and silicon atom of ≡Si–OH group close to 2.358 Å that means its decrease from 3.713 Å in the structure *5*.

And finally, the water molecule coordinated to $(\equiv Si–O–)_2Mo(=O)_2$ species in structure *7* is eliminated that resulted in structure *8* related to $(\equiv Si–O–)_2Mo(=O)_2$ group and releasing of water molecule (the relative energy of the system appeared to be reduced to -337 kJ/mol).

CONCLUSIONS

The undertaken simulation of the reaction of MoO_3 molecule with ≡Si–OH groups of $Si_{10}O_{12}(OH)_{16}$ cluster $Si_{10}O_{12}(OH)_{16} + MoO_3 \rightarrow Si_{10}O_{12}(OH)_{14}O_2MoO_2 + H_2O$ in the temperature interval of 300–1100 K confirms that molybdena dispergation on silica support surface can occur as the result of the formation of the energetically favourable $(\equiv Si–O–)_2Mo(=O)_2$ Mo(VI) oxo-species.

At 700 K, when molybdena dispergation over silica surface begins, the Gibbs energy of the formation of $(\equiv Si–O–)_2Mo(=O)_2$ Mo(VI) oxo-species via reaction of MoO_3 molecule with nearby and distant ≡Si–OH groups of $Si_{10}O_{12}(OH)_{16}$ cluster was found to be -260 and -337 kJ/mol, respectively.

The proposed mechanism of the reaction of MoO_3 molecule with distant ≡Si–OH groups of $Si_{10}O_{12}(OH)_{16}$ cluster at 700 K proceeds in two stages and requires overcoming of the activation barriers of 161 and 154 kJ/mol.

Механізм диспергування MoO_3 на поверхні SiO_2

Д.Б. Насєдкін, А.Г. Гребенюк, Л.Ф. Шаранда, Ю.В. Плюто

Інститут хімії поверхні ім. О.О. Чуйка Національної академії наук України
вул. Олега Мудрака, 17, Київ, 03164, Україна, dmytro.nasiedkin@isc.gov.ua

Диспергування оксиду молібдену на поверхні кремнезему шляхом термічної обробки сухих сумішей MoO_3 та дисперсного кремнеземного носія є зручним препаративним методом синтезу поверхневих оксо-частинок Mo(VI). Рушійною силою термічно індукованого диспергування об'ємного MoO_3 є зменшення поверхневої енергії, яка нижча для поверхневих оксо-частинок Mo(VI). Метою цього дослідження є квантовохімічне моделювання механізму взаємодії молекули MoO_3 з ≡Si–OH групами поверхні кремнезему через реакцію $2(\equiv Si–OH) + MoO_3 \rightarrow (\equiv Si–O–)_2Mo(=O)_2 + H_2O$, що призводить до утворення $(\equiv Si–O–)_2Mo(=O)_2$ оксо-частинок Mo(VI). Був використаний обмежений метод Хартрі-Фока (наближення МО ЛКАО) з використанням валентного базисного набору SBKJC (Stevens-Basch-Krauss-Jasien-Cundari). Кластер $Si_{10}O_{12}(OH)_{16}$ було використано як модель високогідроксильованої поверхні кремнезему, в якій атоми кремнію в основних силоксанових ланцюгах насичені чотирма силанольними та шістьма силандіоловими групами. Такий кластер розглядався як такий, що забезпечує реалістичну структуру для поверхні SiO_2 та демонструє високу стабільність завдяки своєму великому розміру. У розрахунках було використано оптимізовану геометрію молекули MoO_3 симетрії C_{3v}. Було проведено квантовохімічне моделювання реакції $Si_{10}O_{12}(OH)_{16} + MoO_3 \rightarrow Si_{10}O_{12}(OH)_{14}O_2MoO_2 + H_2O$, що супроводжується утворенням поверхневих $(\equiv Si–O–)_2Mo(=O)_2$ оксо-частинок Mo(VI). Ми розглянули дві структури $(\equiv Si–O–)_2Mo(=O)_2$ оксо-частинок Mo(VI), приєднаних до кластера кремнезему $Si_{10}O_{12}(OH)_{16}$ через близькі та віддалені ≡Si–OH групи. При 700 K, коли починається диспергування оксиду молібдену на поверхні кремнезему, енергія Гіббса утворення $(\equiv Si–O–)_2Mo(=O)_2$ оксо-частинок Mo(VI) шляхом реакції молекули MoO_3 з близькими та віддаленими ≡Si–OH групами кластера $Si_{10}O_{12}(OH)_{16}$ становила -260 та -337 кДж/моль відповідно. Механізм реакції молекули MoO_3 з віддаленими ≡Si–OH групами кластера $Si_{10}O_{12}(OH)_{16}$, що супроводжується утворенням $(\equiv Si–O–)_2Mo(=O)_2$ оксо-частинок Mo(VI), був розглянутий як більш енергетично вигідний. Було показано, що при 700 K реакція відбувається у два етапи та вимагає подолання активаційних бар'єрів 161 та 154 кДж/моль.

***Ключові слова**: квантовохімічне моделювання, кремнезем, оксид молібдену, поверхневе диспергування, механізм реакції*

REFERENCES

1. Knözinger H., Taglauer E. 2.4.7 Spreading and Wetting. In: *Handbook of Heterogeneous Catalysis.* (Weinheim: Wiley-VCH Verlag GmbH & Co. KgaA, 2008).
2. Braun S., Appel L.G., Camorim V.L., Schmal M. Thermal Spreading of MoO_3 onto Silica Supports. *J. Phys. Chem. B*. 2000. **104**(28): 6584.
3. Braun S., Appel L.G., Schmal M. Molybdenum species on alumina and silica supports for soot combustion. *Catal. Commun*. 2005. **6**(1): 7.
4. Shi W., Cai X., Wei J., Ma J., Hu T., Wu N., Xie Y. EXAFS study of molybdenum oxide on the structure Al_2O_3. *Surf. Interface Anal*. 2001. **32**(1): 202.
5. Mosqueira L., Fuentes G.A. Molecular selection of MoO_x species during migration on Al_2O_3 and zeolites Y and ZSM-5. *Mol. Phys*. 2002. **100**(19): 3055.
6. Mosqueira L., Gómez S.A., Fuentes G.A. Characterization of MoO_x species on γ-Al_2O_3, Y and ZSM-5 zeolites during thermally activated solid–solid synthesis. *J. Phys.: Condens. Matter.* 2004. **16**(2): S2319.
7. Debecker D.P., Stoyanova M., Rodemerck U., Eloy P., Léonard A., Su B.-L., Gaigneaux E.M. Thermal Spreading as an Alternative for the Wet Impregnation Method: Advantages and Downsides in the Preparation of $MoO_3/SiO_2{-}Al_2O_3$ Metathesis Catalysts. *J. Phys. Chem. C.* 2010. **114(**43): 18664.
8. Debecker D.P., Stoyanova M., Rodemerck U., Gaigneaux E.M. Facile preparation of MoO_3/SiO_2-Al_2O_3 olefin metathesis catalysts by thermal spreading. In: *Studies in Surface Science and Catalysis*. **175**. Proc. 10th Int. Symp. (July 11–15, 2010, Louvain-la-Neuve, Belgium), pp. 581–585.
9. Li Zh., Gao L., Zheng Sh. Investigation of the dispersion of MoO_3 onto the support of mesoporous silica MCM-41. *Appl. Catal., A.* 2002. **236**(1–2): 163.
10. Li Zh., Gao L., Zheng Sh. SEM, XPS, and FTIR studies of MoO_3 dispersion on mesoporous silicate MCM-41 by calcination. *Mater. Lett*. 2003. **57**(29): 4605.
11. Sampieri A., Pronier S., Blanchard J., Breysse M., Brunet S., Fajerwerg K., Louis C., Pérot G. Hydrodesulfurization of dibenzothiophene on MoS_2/MCM-41 and MoS_2/SBA-15 catalysts prepared by thermal spreading of MoO_3. *Catal. Today*. 2005. **107–108**: 537.
12. Mosqueira L., Angeles-Chavez C., Torres-García E. Thermal spreading of MoO_3 in H–ZY. *Mater. Chem. Phys*. 2011. **126**(3): 930.
13. Balcar H., Kubů M., Žilková N., Shamzhy M. MoO_3 on zeolites MCM-22, MCM-56 and 2D-MFI as catalysts for 1-octene metathesis. *Beilstein J. Org. Chem.* 2018. **14**: 2931.
14. Balcar H., Topka P., Žilková N., Pérez-Pariente J., Čejka J. Metathesis of linear α-olefins with MoO_3 supported on MCM-41 catalyst. *Stud. Surf. Sci. Catal.* 2005. **156**: 795.
15. Balcar H., Čejka J. Mesoporous Molecular Sieves as Supports for Metathesis Catalysts. In: *Metathesis Chemistry. NATO Science Series.* **243**. (Dordrecht: Springer, 2007). pp. 151–166.
16. Günther S., Gregoratti L., Kiskinova M., Taglauer E., Grotz P., Schubert U.A. Knözinger H. Transport mechanisms during spreading of MoO_3 on Al_2O_3 supports investigated by photoelectron spectromicroscopy. *J. Chem. Phys*. 2000. **112**(12): 5440.
17. Günther S., Esch F., Gregoratti L., Barinov A., Kiskinova M., Taglauer E., Knözinger H. Gas-Phase Transport during the Spreading of MoO_3 on Al_2O_3 Support Surfaces: Photoelectron Spectromicroscopic Study. *J. Phys. Chem. B*. 2004. **108**(38): 14223.
18. Xu W., Yan J., Wu N., Zhang H., Xie Y., Tang Y., Zhu Y., Yao W. Diffusing behavior of MoO_3 on Al_2O_3 and SiO_2 thin films. *Surf. Sci*. 2000. **470**(1–2): 121.
19. Xu W., Xu J., Wu N., Yan J., Zhu Y., Huang Y., He W., Xie Y. Study of the diffusion behaviour of MoO_3 and ZnO on oxide thin films by SR-TXRF. *Surf. Interface Anal*. 2001. **32**(1): 301.
20. Haber J. Molybdenum Compounds in Heterogeneous Catalysis. *Stud. Inorg. Chem.* 1994. **19**: 477.
21. Fierro J.L.G., Mol J.C. Metathesis of Olefins on Metal Oxides. In: *Metal Oxides: Chemistry and Applications.* (Boca Raton: CRC Press, 2006).
22. Bañares M.A., Mestl G. Chapter 2 Structural Characterization of Operating Catalysts by Raman Spectroscopy. *Adv. Catal.* 2009. **52**: 43.
23. Lwin S., Wachs I.E. Olefin Metathesis by Supported Metal Oxide Catalysts. *ACS Catal.* 2014. **4**(8): 2505.
24. Li L., Scott S.L. X-ray Absorption Spectroscopy Investigation into the Origins of Heterogeneity in Silica-Supported Dioxomonomolybdates. *J. Phys. Chem. C.* 2021. **125**(42): 23115.
25. Savinelli R.O., Scott, S.L. Wavelet transform EXAFS analysis of mono- and dimolybdate model compounds and a Mo/HZSM-5 dehydroaromatization catalyst. *Phys. Chem. Chem. Phys*. 2010. **12**(21): 5660.
26. Yamamoto K., Chan K.W., Mougel V., Nagae H., Tsurugi H., Safonova O.V., Mashima K., Copéret C. Silica-supported isolated molybdenum di-oxo species: formation and activation with organosilicon agent for olefin metathesis. *Chem. Commun*. 2018. **54**(32): 3989.

27. Berkson Z.J., Bernhardt M., Schlapansky S.L., Benedikter M.J., Buchmeiser M.R., Price G.A., Sunley G.J., Copéret Ch. Olefin-Surface Interactions: A Key Activity Parameter in Silica-Supported Olefin Metathesis Catalysts. *JACS Au.* 2022. **2**(3): 777.
28. Berkson Z.J., Zhu R., Ehinger Ch., Lätsch L., Schmid S.P., Nater D., Pollitt S., Safonova O.V., Björgvinsdóttir S., Barnes A.B., Román-Leshkov Y., Price G.A., Sunley G.J., Copéret Ch. Active Site Descriptors from ^{95}Mo NMR Signatures of Silica-Supported Mo-Based Olefin Metathesis Catalysts. *J. Am. Chem. Soc.* 2023. **145**(23): 12651.
29. Guo C.S., Hermann K., Hävecker M., Thielemann J.P., Kube P., Gregoriades L.J., Trunschke A., Sauer J., Schlögl R. Structural Analysis of Silica-Supported Molybdena Based on X-ray Spectroscopy: Quantum Theory and Experiment. *J. Phys. Chem. C*. 2011. **115**(31): 15449.
30. Handzlik J., Kurleto K., Gierada M. Computational Insights into Active Site Formation during Alkene Metathesis over a MoO_x/SiO_2 Catalyst: The Role of Surface Silanols. *ACS Catal*. 2021. **11**(21): 13575.
31. Kurleto K., Tielens F., Handzlik J. Isolated Molybdenum(VI) and Tungsten(VI) Oxide Species on Partly Dehydroxylated Silica: A Computational Perspective. *J. Phys. Chem. C*. 2020. **124**(5): 3002.
32. Nasiedkin D.B., Nazarchuk M.O., Grebenyuk A.G., Sharanda L.F., Plyuto Yu.V. Quantum Chemical Simulation of MoO_3 Dispergation on Hydroxylated SiO_2 Surface. *Surface.* 2021. **13(28)**: 75.
33. Schmidt M.W., Baldridge K.K., Boatz J.A., Elbert S.T., Gordon M.S., Jensen J.H., Koseki S., Matsunaga N., Nguyen K.A., Su S., Windus T.L., Dupuis M., Montgomery J.A. General atomic and molecular electronic structure system. *J. Comput. Chem*. 1993. **14**(11): 1347.
34. Barca G., Bertoni C., Carrington L., Datta D., De Silva N., Deustua J.E., Fedorov D.G., Gour J.R., Gunina A.O., Guidez E., Harville T., Irle S., Ivanic J., Kowalski K., Leang S.S., Li H., Li W., Lutz J.J., Magoulas I., Mato J., Mironov V. Recent developments in the general atomic and molecular electronic structure system. *J. Chem. Phys*. 2020. **152**(15): 154102.
35. Khavryutchenko V., Sheka E. Computer modeling of amorphous silica structures. *React. Kinet. Catal. Lett*. 1993. **50**(1–2): 389.
36. Khavryuchenko V.D., Sheka E.F. Computational modeling of amorphous silica. 2. Modeling the initial structures. Aerosil. *Journal of Structural Chemistry*. 1994. **35**(3): 291.
37. Peacor D.B. High-temperature single-crystal study of the cristobalite inversion. *Zeitschrift für Kristallographie – Crystalline Materials.* 1973. **138**(1–6): 274.
38. Wright A.F., Leadbetter A.J. The structures of the β-cristobalite phases of SiO_2 and $AlPO_4$, The Philosophical Magazine. *A Journal of Theoretical Experimental and Applied Physics*. 1975. **31**(6): 1391.
39. Papakondylis A., Sautet Ph. Ab Initio Study of the Structure of the α-MoO_3 Solid and Study of the Adsorption of H_2O and CO Molecules on its (100) Surface. *J. Phys. Chem.* 1996. **100**(25): 10681.
40. Zhou M., Andrews L. Infrared spectra and density functional calculations of the CrO_2^-, MoO_2^-, and WO_2^- molecular anions in solid neon. *J. Chem. Phys.* 1999. **111**: 4230002E.
41. Spiridonov V.P., Zasorin E.Z. Modern High-Temperature Electron Diffraction. In: *Characterization of High Temperature Vapors and Gases.* Proc. 10th Materials Research Symposium at the National Bureau of Standards, (September 18–22, 1978, Gaithersburg, Maryland). (NBS Special Publication 561, V. 1. U.S. Dep. of Commerce, Nat. Bureau of Standards, 1979). pp. 711–755.
42. *J. Phys. Chem. Ref. Data,* Monograph 9. NIST-JANAF Thermochemical Tables. Part I and Part II. Fourth Edition (Chase M.W., Jr., Ed). National Institute of Standards and Technology, Gaithersburg, USA, 1998, p. 1593.

Received 16.03.2025, accepted 04.09.2025